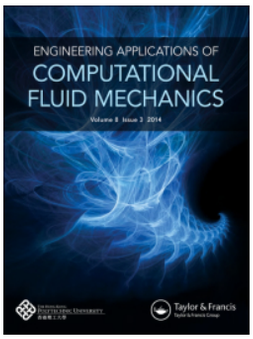

Engineering Applications of Computational Fluid Mechanics

ISSN: (Print) (Online) Journal homepage: www.tandfonline.com/journals/tcfm20

Online prediction of ship maneuvering motions based on adaptive weighted ensemble learning under dynamic changes

Yaohui Yu, Hongbin Hao, Zihao Wang, Yan Peng & Shaorong Xie

To cite this article: Yaohui Yu, Hongbin Hao, Zihao Wang, Yan Peng & Shaorong Xie (2024) Online prediction of ship maneuvering motions based on adaptive weighted ensemble learning under dynamic changes, Engineering Applications of Computational Fluid Mechanics, 18:1, 2341922, DOI: 10.1080/19942060.2024.2341922

To link to this article: https://doi.org/10.1080/19942060.2024.2341922

Published online: 16 Apr 2024.

ENGINEERING APPLICATIONS OF COMPUTATIONAL FLUID MECHANICS
2024, VOL. 18, NO. 1, 2341922
https://doi.org/10.1080/19942060.2024.2341922

Taylor & Francis
Taylor & Francis Group

Online prediction of ship maneuvering motions based on adaptive weighted ensemble learning under dynamic changes

Yaohui Yu[a], Hongbin Hao[b], Zihao Wang [a,c], Yan Peng[a,c] and Shaorong Xie[c,d]

[a]School of Artificial Intelligence, Shanghai University, Shanghai, People's Republic of China; [b]Department of Civil and Environment Engineering, The Hong Kong Ploytechnic University, Kowloon, Hong Kong Special Administrative Region, Hong Kong, People's Republic of China; [c]Engineering Research Center of Unmanned Intelligent Marine Equipment, Ministry of Education, Shanghai, People's Republic of China; [d]School of Computer Engineering and Science, Shanghai University, Shanghai, People's Republic of China

ABSTRACT

Dynamic changes in ship maneuverability challenge the accuracy and effectiveness of ship maneuvering models. This paper proposes an online prediction method based on the adaptive weighted ensemble learning framework, which can adaptively update the model according to changes in maneuverability, especially for reoccurring changes. The method contains two main mechanisms: the change monitoring mechanism and the adaptive weighting mechanism. The former identifies the change in ship dynamics and decides when to incorporate a new base model; the latter adjusts the weights of the base models to align with current scenarios, thus ensuring the predictive accuracy. To assess the method's effectiveness under varying ship dynamics, the online prediction of ship maneuvering motions under speed-induced dynamic changes is investigated. Compared with the offline model, the result demonstrates the superiority of the adaptive weighted ensemble model. The proposed method can consistently provide accurate predictions in the scenarios with reoccurring changes, and can also enhance the model capability by adjusting weights to cope with some unencountered changes.

ARTICLE HISTORY
Received 28 December 2023
Accepted 5 April 2024

KEYWORDS
Online prediction; ensemble learning; concept drift; non-stationary environments; autonomous ship; ship maneuvering motion

1. Introduction

Accurate predictive models of ship maneuvering motion are crucial for decision support systems (Wu et al., 2022) and digital twins (Hatledal et al., 2020; Nielsen et al., 2022) in maritime operations. This importance has been rising with the advancement of Maritime Autonomous Surface Ships (MASS). However, established models may fail under real-world conditions due to changes in ship loading conditions (Lan et al., 2023; Yasukawa et al., 2022), navigational patterns (Okuda et al., 2023), and external environmental factors (Wang et al., 2021). Therefore, adaptable modelling that can handle changes in ship maneuverability is particularly important.

The data-driven modelling method based on navigation data has the potential to handle ship dynamic changes (PANDA, 2023). This approach is less time-consuming than the widely used captive model tests and computational fluid dynamics (CFD) techniques (Liu et al., 2018; Xiang et al., 2023). In addition, the data-driven method can be applied to full-scale ships without the constraints of large specialized facilities and computational resources. This efficiency and flexibility make it more beneficial for adaptive modelling under varying dynamic characteristics.

In the realm of data-driven modelling, there are two primary modes: online and offline. Offline models are static, built from a predetermined dataset to capture specific dynamic features (Silva & Maki, 2022; Wakita et al., 2022; Wang et al., 2020; Wang et al., 2022; Xue et al., 2021). In contrast to offline models, online models are dynamics, timely updating with incoming data to maintain accuracy, thus effectively addressing changes in dynamic characteristics. Many scholars have explored online modelling algorithms to achieve the timely updating of ship maneuvering models. For example, Yue et al. (2022) proposed an adaptive update law based on truncated integral filter regression, which enables the model parameters to be updated online. Wang et al. (2022) proposed a real-time parameter identification method based on nonlinear Gaussian filtering for a nonlinear response model. This approach is verified based on the simulation data of the Mariner ship's zigzag maneuvers. Xu et al. (2019) used incremental least squares support vector machines (LSSVM) to identify parameters in the nonlinear response model and conducted a comparative analysis with offline method. Ouyang and Zou (2021) proposed a sliding window method based on Gaussian process regression to improve the adaptability of models.

CONTACT Zihao Wang zihaowang@shu.edu.cn

In addition, Pei et al. (2023) proposed an online prediction framework based on the least square-twin support vector machine with an event-triggered mechanism for underwater vehicles. The above studies mainly explored online modelling from an algorithmic design perspective, while their algorithm evaluations were constrained to scenarios with constant conditions.

Addressing scenarios with changing dynamic characteristics, Wang et al. (2022) developed an adaptive predictor using incremental Gaussian Process regression, testing it through simulations of 20°/20° zigzag maneuvers under dynamic ocean conditions. Chen et al. (2023) introduced a sliding window based LSSVM method for modelling ship motions with four degrees of freedom (DOF), and a simulation test is conducted under variable wave conditions. Both studies employed an error detection mechanism to determine the appropriate time for model updates. In the previous study, Yu et al. (2023, June 11) analyzed two popular online learning patterns, i.e. incremental learning and sliding window, under varying loading conditions. The results show that both incremental learning and sliding windows can ultimately update the model under varying loading conditions. However, the accuracy of the updated model cannot be guaranteed without acquiring sufficient new data.

Overall, the effectiveness of the above online modelling strategies relies on the accumulation of sufficient samples. This process typically requires a long time, leading to a slow adaptation to large changes. Nevertheless, changes in dynamic characteristics are sometimes repetitive. In such reoccurring scenarios, the online modelling methods still require continuous retraining to readapt to the current dynamics. This leads to repeat updating or training of models, resulting in significant consumption of time and resources.

Adaptive ensembles have proven its value as an effective way to cope with non-stationary environments. As developed from the online version of ensemble learning, adaptive ensembles typically employ the following strategies (Polikar, 2012): (1) adaptation of the model's weights; (2) adaptation of the model's parameters; (3) creation and addition of new models to the ensemble. Despite the demonstrated value of adaptive ensembles, there are fewer adaptive ensemble studies focusing on regression tasks. For instance, Kadlec and Gabrys (2011) introduced an incremental soft sensing regression algorithm using a sliding window technique, where process changes are detected by t-tests, and models are dynamically updated and weighted based on window data. Kaneko and Funatsu (2014) proposed an adaptive ensembles method based on multiple support vector regression models, periodically updated and weighted by the latest data window. Gomes Soares and Araújo (2015) proposed an online weighted ensemble model for regression problems, which integrates on-line inclusion and removal of models, dynamic adaptation of model's weights based on recent predictions, and on-line adjustment of model's parameters.

To quickly adapt to ship dynamic changes and enhance model applicability, this study proposes an adaptive weighted ensemble learning framework with fast adaptation capability, especially for handling scenarios with reoccurring ship dynamics. To validate the effectiveness of the proposed online prediction method, test scenarios are created where changes in ship maneuverability are induced by variations in ship navigation speed and these changes are assumed to be unforeseen. The adaptive weighted ensemble model and the offline model are tested and compared with zigzag and turning maneuvers. The results demonstrate that the proposed approach can address the need for rapid response to changes and also broaden the potential model capability.

This work is organized as follows: Section 2 presents the problem formulation for online modelling of changes in ship dynamics. The adaptive weighted ensemble learning framework for ship maneuvering motions is designed in detail in Section 3. The experimental design and results are shown in Section 4. The conclusions are drawn in Section 5.

2. Problem formulation

Changes in ship maneuverability, influenced by varying load conditions, navigational patterns, and external conditions, can lead to inaccuracies in previously established models over time. In the field of machine learning, this phenomenon is identified as *concept drift*, which refers to the statistical properties of the target domain change over time in a dynamic or non-stationary environment (Gama et al., 2014). Formally, concept drift can be described as follows (Lu et al., 2018).

Given a time period $T_{0,t} = [0, t]$, a set of samples denotes as $S_{0,t} = \{d_0, \ldots, d_t\}$, where $d_i = (X_i, y_i)$ is a group of observations at a certain time, containing a feature vector X_i and output y_i. Assuming that $S_{0,t}$ follows a certain distribution $F_{T_{0,t}}(X, y)$, concept drift occurs from the timestamp $t+1$, resulting in $F_{T_{0,t}}(X, y) \neq F_{T_{t+1,\infty}}(X, y)$. This can also be expressed as $\exists t : P_t(X, y) \neq P_{t+1}(X, y)$, where $P_t(X, y)$ denotes the joint probability of X and y at timestamp t. According to the rate and manner of data distribution change, concept drift can be divided into four types: sudden drift, gradual drift, incremental drift and reoccurring concepts, as shown in Figure 1.

In general, the ship maneuvering model can be denoted as a function $\hat{f} : Z \rightarrow Y$ that maps a feature

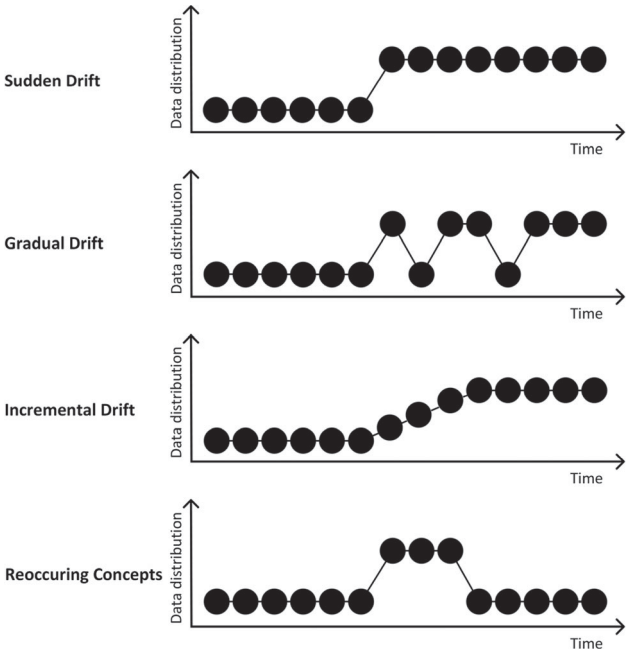

Figure 1. Types of concept drift (Gama et al., 2014).

vector X_i ($X_i \in Z$) to an output vector y_i ($y_i \in Y$), where $Z \subseteq \mathbb{R}^d$ denotes the domain of the features and $Y \subseteq \mathbb{R}^{d'}$ denotes the domain of the outputs, with dimensions $d, d' \in \mathbb{N}$. Assuming that the ship dynamics in the current period T_c can be adequately characterized as a function f_{T_c}, we can construct a model $\hat{f}_{T_c}$ to approximate f_{T_c} by minimizing the $Error(\hat{f}_{T_c}, f_{T_c})$. However, when the ship's dynamic characteristics suffer a concept drift at the period T_{new} that changes f_{T_c} to $f_{T_{new}}$, the $\hat{f}_{T_c}$ will not be able to meet the accuracy requirements for the task at hand. At this time, an online modelling approach is expected to adjust the model $\hat{f}_{T_c}$ to approximate $f_{T_{new}}$. In this paper, the concept drift occers within the normal range of ship maneuvers, excluding hazardous behaviours. The reoccurring concept refers to the repetition of dynamic characteristics. For instance, when the ship dynamic changes from state A to state B and then repeats to state A, it exemplifies a reoccurring concepts.

In real-world ship navigation, the concept drift in ship maneuverability may be a combination of different types of concept drift. For the first three types of concept drift in Figure 1, the model needs to be updated to accommodate these drifts, while reoccurring concepts can be quickly adapted by reusing previous models.

To balance the accuracy and responsiveness of the model under concept drift, this study aims to design an ensemble learning framework with real-time adjustment of weights. This involves both adapting to unknown concept drift and reusing previous models for reoccurring concepts. The basic idea is to create models for specific conditions as base models and combine the predictions by adjusting the weights of the base models online, thus enhancing the adaptive capacity of the ensemble model. The ensemble model $\hat{f}_{ensemble}$ is expressed as:

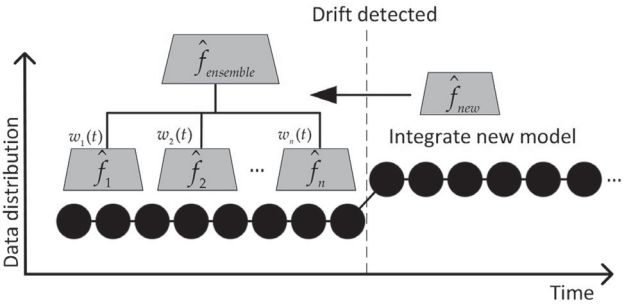

Figure 2. Online construction and prediction of ensemble model.

$$\hat{f}_{ensemble}(X_i) = w_1\hat{f}_1(X_i) + w_2\hat{f}_2(X_i) + \ldots + w_n\hat{f}_n(X_i) \quad (1)$$

where $\hat{f}_j$ ($j = 1, 2, \ldots, n$) represents the base models and w_j denotes the weight of $\hat{f}_j$. It should be noted that the number of base models n is not fixed. New base models will be created and integrated into the ensemble model when new concept drift is detected. Meanwhile, the weight w_j is dynamically updated during the online prediction process to cope with reoccurring concepts. The schematic is shown in Figure 2.

To establish the aforementioned framework, the main issues involve how to detect concept drift, how to train a new model, and how to adjust the weights of base models to quickly adapt to reoccurring concepts. The following section will explore specific solutions to these challenges.

3. Adaptive weighted ensemble learning framework

The establishment of the adaptive weighted ensemble learning framework lies in the online construction of ensemble models and the design of adaptive strategies. Ensemble learning is considered to be an effective way to deal with concept drift, especially reoccurring concepts. It combines the predictions of multiple base models to improve the final prediction. As base models store the information about historical concepts, a reasonable combination strategy enables the effective recalling of the corresponding models for reoccurring concepts.

3.1. Overview of the framework

For the specific problem of ship maneuvering modelling, the change monitoring mechanism, the online

batch integration modelling approach, and the adaptive weighting mechanism are designed. To cope with the concept drift during ship navigation, the change monitoring mechanism continuously monitors dynamic changes by the prediction bias of the ensemble model. Upon the detection of the concept drift, a new base model is created using an online batch modelling approach, and the base model is then integrated into the ensemble model. Furthermore, the weights of base models are dynamically adjusted according to the current scenario based on the adaptive weighting mechanism.

The workflow of the adaptive weighted ensemble learning framework for ship maneuvering modelling is shown in Figure 3. The specific phases are as follows:

(1) Modeling and Integration Phase: To characterize unknown nonlinear dynamic features, a data-driven algorithm creates a base model using a batch sliding window. Subsequently, the base model is integrated into the ensemble model.
(2) Change Monitoring Phase: The developed ensemble model provides multi-step iterative predictions from a previous moment to the current moment. The cumulative deviation E^t is utilized to ascertain the occurrence of the concept drift. If changes are detected, the process will revert to the Modeling and Integration Phase (1). Otherwise, the procedure transitions into the Weights Adjustment Phase (3).
(3) Weights Adjustment Phase: To make the model have a better performance in the present, this phase adaptively adjusts the weights of base models. After updating weights, the procedure goes back to the Change Monitoring Phase (2) at the next time step and proceeds to iterate. Meanwhile, online predictions of ship maneuvering motions can be performed if a prediction task is required.

By following the above workflow, the model can be updated online to ensure accurate predictions of ship maneuvering motions during ship navigation.

The adaptive weighted ensemble learning algorithm is specifically described in Algorithm 1.

The algorithm starts at step 1 with data stream D as input, defining the size of the data window W and the error window N, as well as the error threshold K_e for adding a new model. In step 2, a series of variables are initialized, including the set of models $\mathcal{E}$, the number of models k, and time t. D^t and d^t represent the data window and the error window at time t, respectively. The new model f_k trained with D^t is obtained at step 3, and it is added to $\mathcal{E}$ after setting k and the weight w_k.

The online phase of the algorithm runs from step 4 to step 5. The windows slide by 1 time step every time

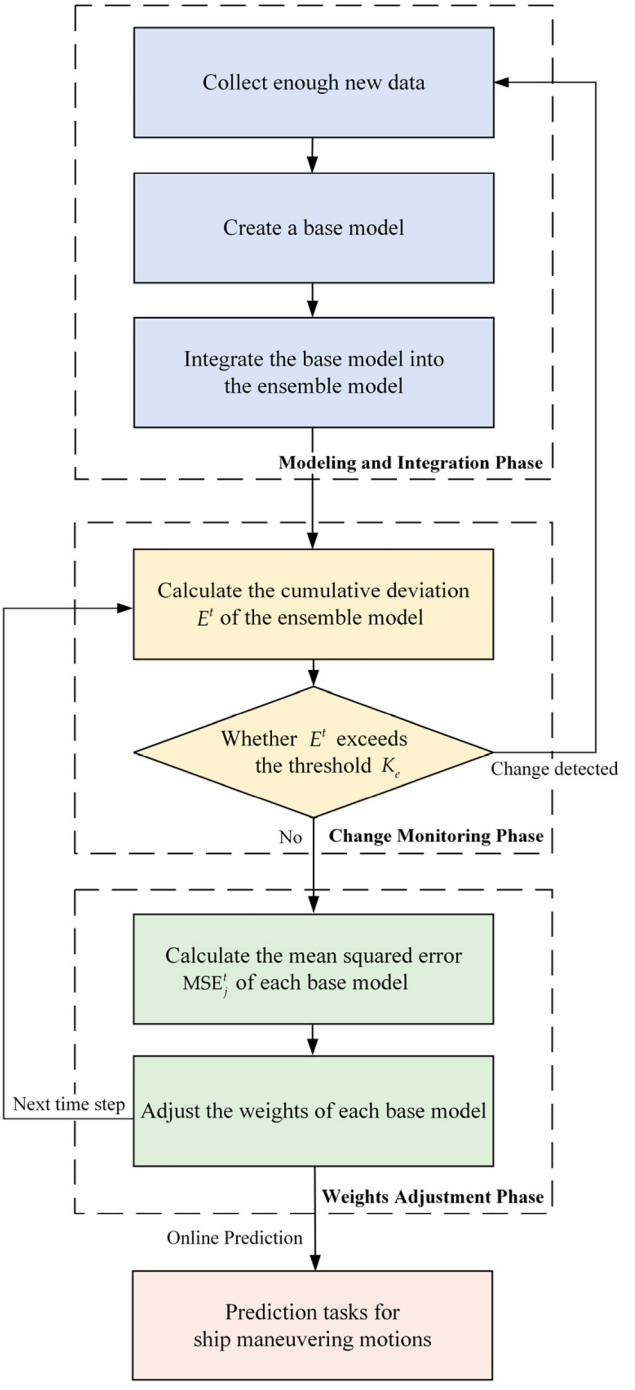

Figure 3. The workflow of the adaptive weighted ensemble learning framework.

a new sample (X_t, y_t) is received (step 4a). New sample is added to the window and old sample is removed from the window. The prediction $\hat{y}_t$ of the ensemble model is calculated and the deviation is judged (step 4b and step 4c). If the prediction deviation exceeds the set threshold K_e, step 4c (i) and step 4c (ii) are executed. The windows slide by m time steps to update D^t and d^t, a new model f_0 is trained with D^t, and it is added to $\mathcal{E}$ after setting k, w_k and f_k. Conversely, if the prediction meets the accuracy

Algorithm 1: Adaptive weighted ensemble learning

1. **Input:** data stream $\mathrm{D} = \{(X_t, y_t)|X_t \in \mathbb{R}^r, y_t \in \mathbb{R}, t = 1, 2, \ldots\}$; data window's size, W; error window's size, N; error threshold to add a new model, K_e;
2. **Initialization:** set of models $\mathcal{E} \leftarrow \emptyset$; number of models $k = 0$; time $t = W$; data window $\mathrm{D}^t = \{(X_i, y_i)\}_{i=1}^{W} \subset \mathrm{D}$; error window $\mathrm{d}^t = \{(X_j, y_j)\}_{j=W-N+1}^{W} \subset \mathrm{D}^t$;
3. $f_k \leftarrow$ obtain a new model trained with D^t; set $k \leftarrow k + 1$, $w_k = 1$ and $\mathcal{E} \leftarrow \mathcal{E} \cup f_k$;
4. **while** true **do**:
   (a) slide windows by 1 time step: $t \leftarrow t + 1$; $\mathrm{D}^t = \mathrm{D}^{t-1} + (X_t, y_t) - (X_{t-W}, y_{t-W})$; $\mathrm{d}^t = \mathrm{d}^{t-1} + (X_t, y_t) - (X_{t-N}, y_{t-N})$;
   (b) predict y_t as: $\hat{y}_t = \left(\sum_{j=1}^{k} w_j f_j(X_t)\right) / \sum_{j=1}^{k} w_j$;
   (c) if $|(\hat{y}_t - y_t)/y_t| > K_e$
      (i) slide windows by W time step: $t \leftarrow t + W$;
      (ii) $f_0 \leftarrow$ obtain a new model trained with D^t; set $k \leftarrow k + 1$, $w_k = 1$, $f_k \leftarrow f_0$, and $\mathcal{E} \leftarrow \mathcal{E} \cup f_k$;
   (d) obtain MSE_j^t for each model $f_j \in \mathcal{E}$ on d^t;
   (e) weight all models from $\mathcal{E}$ with MSE_j^t;
5. **end while**

requirement, the weights of the models are updated (step 4d and step 4e). The mean square error MSE_j^t of each model $f_j \in \mathcal{E}$ at time t is obtained on d^t, and the weights of all models are assigned with MSE_j^t.

3.2. Change monitoring mechanism

The established model may no longer be able to provide accurate predictions when ship dynamics change, which is externally reflected as excessive model prediction errors. The change monitoring mechanism is designed to detect the concept drift of ship dynamic characteristics and thus determine when to create a new base model to expand model capabilities. The cumulative deviation of predictions relative to actual values is used as an evaluation indicator for the change monitoring mechanism.

Assumed that there are n base models in the ensemble model: $f_1, f_2, \ldots, f_n$, where each base model contains three degrees of freedom as $f_n = \{f_{n,u}, f_{n,v}, f_{n,r}\}$, comprising the surge velocity u, sway velocity v, and yaw rate r, respectively. The final prediction $\hat{u}_{k+1}$, $\hat{v}_{k+1}$, $\hat{r}_{k+1}$ of the ensemble model for the next time step can be obtained as:

$$\hat{u}_{k+1} = \frac{\sum_{i=1}^{n} w_{i,u} f_{i,u}}{\sum_{i=1}^{n} w_{i,u}}, \tag{2}$$

$$\hat{v}_{k+1} = \frac{\sum_{i=1}^{n} w_{i,v} f_{i,v}}{\sum_{i=1}^{n} w_{i,v}}, \tag{3}$$

$$\hat{r}_{k+1} = \frac{\sum_{i=1}^{n} w_{i,r} f_{i,r}}{\sum_{i=1}^{n} w_{i,r}}, \tag{4}$$

where $w_{i,u}$, $w_{i,v}$ and $w_{i,r}$ represent the weights of the ith base models in the surge, sway, and yaw rate direction, respectively.

In the multi-step predictions, the predicted values are used as the inputs at the next time step. In other words, an iterative prediction is performed to simulate the ship maneuvering process. Pictorially, this process can be described by Figure 4, where D^t, $P^t(M)$ and E^t represent the collected data, the Mth step predicted value, and the cumulative deviation at time step t, respectively. In details, the cumulative deviation E^t is the absolute percentage error that balances the difference in magnitude between the three degrees of freedom. It is calculated by the following formula:

$$E^t = \left| \frac{P^t(M) - D^t}{D^t} \right| \times 100\% \tag{5}$$

The judgment condition for detecting dynamic changes is represented as:

$$(E_u^t > K_e) \wedge (E_v^t > K_e) \wedge (E_r^t > K_e) \tag{6}$$

where K_e denotes a predefined threshold. If E_u^t, E_v^t and E_r^t all exceed K_e, it implies that the ensemble model cannot meet the requirements of the prediction accuracy at the current moment. At this point, a new model will be created and integrated to expand the capabilities of the ensemble model. The setting of the threshold K_e needs to consider as a trade-off between prediction accuracy and computational demands. Setting a small threshold means that even small changes in dynamics will trigger updates to the model. While this setting ensures that the model stays up-to-date, it may require more computational resources to handle the updates. On the other hand, computational resources can be conserved by setting a higher threshold, but the reduction in prediction accuracy needs to be tolerated at the same time. Hence, it is crucial to establish a reasonable threshold according to the specific application scenarios.

3.3. Online batch integration modelling approach

New base models need to be created to adapt to the changes when changes are detected. Both sample-based learning algorithms and batch-based learning algorithms can be employed to establish a base model online. It is possible to replace the online algorithm in a modular manner. In this study, the batch-based learning is

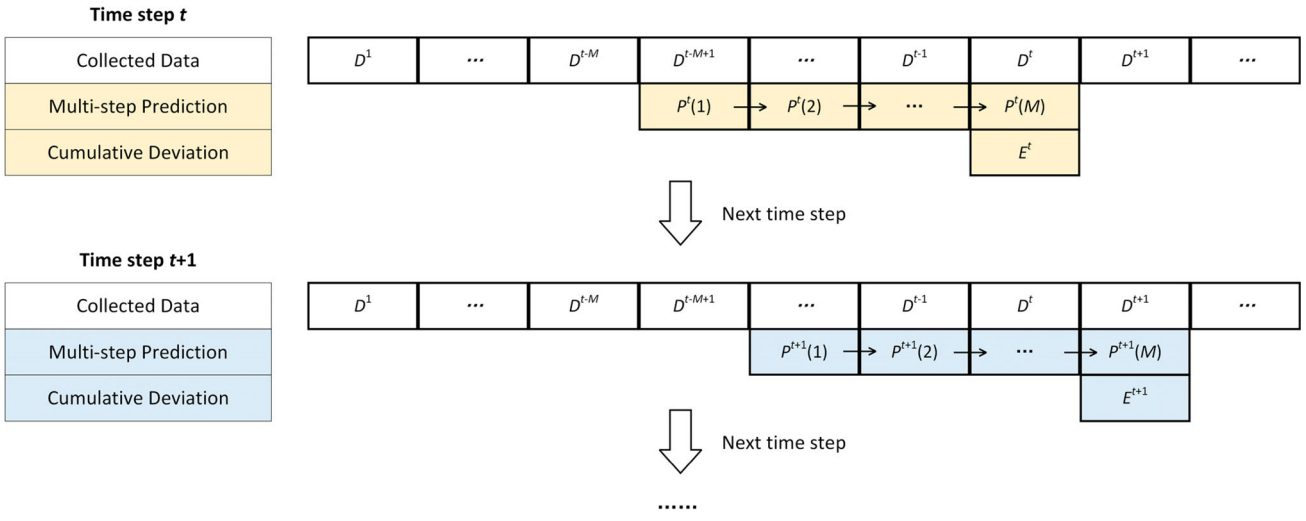

Figure 4. Calculation of cumulative deviation.

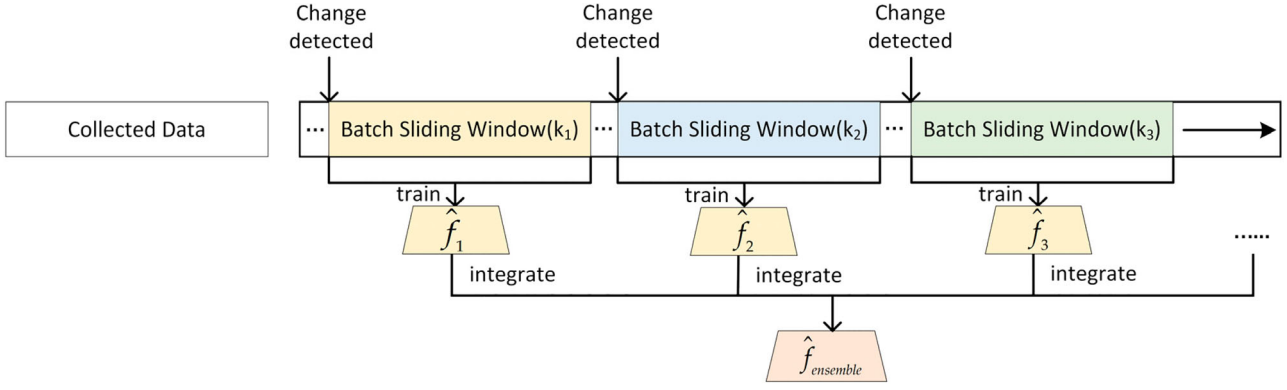

Figure 5. Online construction of the ensemble model.

illustrated as an example in Figure 5. After a change is detected, the data-driven algorithm uses the data in the batch sliding window to create a new base model. Then, the base model is subsequently integrated into the ensemble model.

3.4. Adaptive weighting mechanism

The adaptive weighting mechanism dynamically adjust the weights in Equation (1) based on the prediction errors of each base model. This adjustment allows the ensemble model to adapt to reoccurring scenarios while also using interpolations from existing models to cover scenarios that have not yet been explicitly modelled.

A sliding window of fixed size is used to store multiple one-step prediction errors, as shown in Figure 6. Each base model $\hat{f}_j$ generates a set of errors within N time steps, where each error is a one-step prediction bias. The D^t, $p_j^t(N)$ and $e_j^t(N)$ represent the collected data, the Nth one-step predicted value, and the corresponding square error at time step t, respectively. The sliding window of errors moves as new data are collected and the corresponding errors are calculated, removing old errors while incorporating new ones.

The mean square error MSE_j^t is applied to quantify the performance of the base model $\hat{f}_j$ at time step t, as follows:

$$\mathrm{MSE}_j^t = \frac{1}{N}\sum_{i=1}^{N} e_j^t(i) \tag{7}$$

The weight w_j^t of the model is dynamically adjusted as:

$$w_j^t = \frac{1}{exp(\alpha \cdot \mathrm{MSE}_j^t)}, \tag{8}$$

where α is a predefined error sensitivity factor. Weight adjustments remain relatively even across all base models when α is small, indicating that the process is insensitive to errors at low values of α. Conversely, the well-performing base models have a more significant impact when α is large, while the poor-performing base models do not negatively impact the overall performance of the ensemble model.

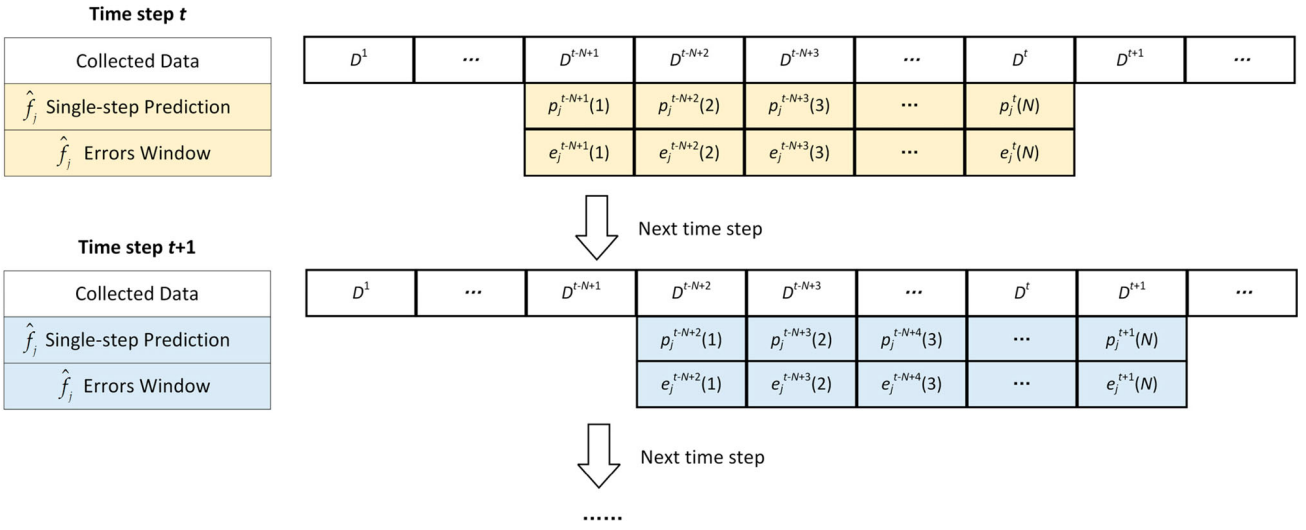

Figure 6. The sliding window of errors for the adaptive weighting mechanism.

Table 1. Principal particulars of KCS.

Parameter		Full-scale
Length between the perpendiculars	L[m]	230.0
Breadth	B[m]	32.2
Draft	d[m]	10.8
Displacement volume	∇[m^3]	52046
Block coefficient	C_b	0.651
Longitudinal coordinate of the centre of gravity	x_G[m]	−3.39
Metacentric height	$\overline{GM}$[m]	0.60
Metacenter height above baseline	$\overline{KM}$[m]	14.1
Propeller diameter	D_p [m]	7.9
Propeller pitch ratio	p	0.997
Number of propeller blades	Z	5
Rudder area including the horn	A_R[m^2]	54.43

Table 2. Vessel speeds across different times.

Time	Speed (knots)
0 ∼ 500s	15.5
500 ∼ 1000s	19.8
1000 ∼ 1500s	24.0
1500 ∼ 2000s	15.5
2000 ∼ 2500s	19.8
2500 ∼ 3000s	24.0
3000 ∼ 3500s	18.1
3500 ∼ 4000s	22.3

4. Experimental design and results

4.1. Test scenario setup: ship maneuvers at varying speeds

To evaluate the performance of online predictions under concept drift, ship maneuver scenarios at different speeds are chosen as test cases. Notably, changes in ship speeds can result in different dynamic characteristics of ship maneuvering motions, which can effectively represent sudden drift and reoccurring concepts during navigation. Additionally, the concept drift is treated as unforeseen information to evaluate the drift detection and adaptation capability of the proposed method.

The KCS container ship is chosen as the object in this study, with its principal characteristics outlined in Table 1. The 3-DOF MMG model (Son & Nomoto, 1981) is employed to generate data and simulations are performed at five navigation speeds: 15.5, 18.1, 19.8, 22.3, and 24.0 knots.

The test scenarios are conducted using 20°/20° zigzag maneuvers and 30° turning maneuvers at varying navigation speeds. These variations in speeds correspond to the concept drift in dynamic characteristics. The speeds

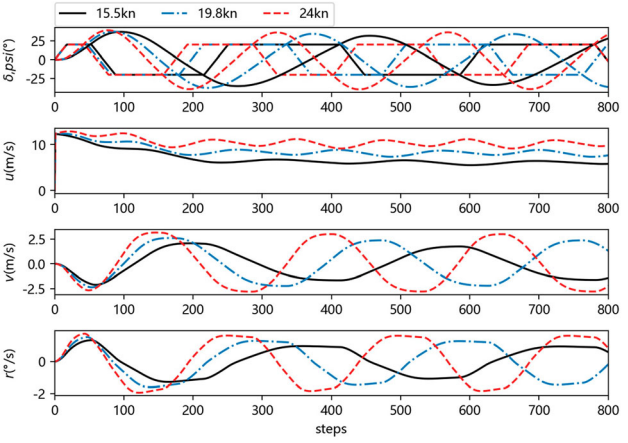

Figure 7. The zigzag maneuvers at 15.5kn, 19.8kn and 24.0kn.

set for different periods are shown in Table 2. The speed changes are produced by altering the propeller revolution. The concept drift occurs at 500, 1000, 1500, 2000, 2500, 3000 and 3500 s, respectively. In this case, the recurrence of speeds represents reoccurring concepts. The simulation time for each scenario is 4000 s, with a data sampling interval of 0.5 s.

Figure 7 illustrates the difference in ship maneuverability at 15.5, 19.8, and 24.0 knots by taking the 20°/20° zigzag maneuver as an example. The overshoot angle

Table 3. Comparisons of zigzag maneuvers at different speeds.

	15.5kn	19.8kn	24.0kn
$1^{st}\psi_{os}$[1](°)	16.9	17.3	19.0
$2^{nd}\psi_{os}$(°)	15.2	17.5	19.2
$3^{rd}\psi_{os}$(°)	11.7	14.3	16.1
$1^{st}t_{os}$[2](s)	50.0	43.0	39.0
$2^{nd}t_{os}$(s)	133.0	111.0	97.0
$3^{rd}t_{os}$(s)	228.0	187.0	161.0

1 Denotes the overshoot angle.
2 Denotes the time to check yaw.

and the time to check yaw are recorded in Table 3. It is evident that the ship maneuverability is significantly influenced by its velocity. At higher navigation speeds, the ship can respond more quickly to steering inputs, which is reflected in the shorter time to reach the overshoot angle, but it also has a greater tendency to deviate from its intended course, resulting in a larger overshoot angle. These changes in dynamic characteristics may lead to the ineffectiveness of the model such as the Abkowitz model, which is based on a Taylor series expansion around the steady state of forward motion with a constant speed. Therefore, it is necessary to update the model to ensure the accuracy of online predictions.

4.2. Approach setup and description

For the data-driven modelling of the base model, a parametric modelling scheme is chosen. The equations of ship maneuvering motion are represented by the Abkowtiz model shown in Appendix A, and parameter estimation is implemented using ordinary least squares (OLS) regression. It is worth noting that this part of the modelling scheme can be replaced by other schemes. The proposed framework is not restricted to specific ship dynamic models or data-driven algorithms.

The following setup is employed for the adaptive weighted ensemble learning method:

Modeling and Integration Phase: The batch sliding window size W is set 500 to align with the data volume requirements for data-driven modelling.

Change Monitoring Phase: The number of multi-step prediction steps M is set to 20 and the absolute percentage error threshold K_e is set to 0.06. This means that the 20th-step predicted value is monitored with a maximum allowable deviation of 6%.

Weights Adjustment Phase: In the case of sudden drifts in variable-speed maneuver simulations, a smaller error window N enables weight assignments to be more responsive to drifts, facilitating a quicker adaptation to changes. N is set to 5, meaning that the error window retains the five most recent one-step prediction errors. The role of α is to control the proportion of weight allocation. To investigate the effect of different weight allocation proportions on the online prediction, α is set to two values of 4000 and 10000 and a comparative study is conducted.

Table 4. Changes detected in variable-speed zigzag.

Order	The step number for the change detected	E_u^t	E_v^t	E_r^t
1	1012	0.0603	0.3905	0.4192
2	2020	0.0774	0.0644	0.4802

In addition, a comparison is made between the online update framework and conventional offline modelling approach. Specifically, the offline model is constructed from the data under a single speed condition, corresponding to the initial base model of the ensemble model.

The Root Mean Square Error (RMSE) is utilized for the evaluation of accuracy through the following formula:

$$\mathrm{RMSE} = \sqrt{\frac{1}{n}\sum_{i=1}^{n}(y_i - \hat{y}_i)^2} \tag{9}$$

where $\hat{y}_i$ denotes the prediction value; y_i is the true value; n is the number of samples.

4.3. Results analysis and discussion

Figure 8 shows the modelling and prediction results of the 20°/20° zigzag maneuvers at varying navigation speeds. As described in Section 4.1, there are seven times of speed alteration. The first two changes activate the change monitoring mechanism, resulting in the creation and integration of a new base model into the ensemble model; these periods in the figure are marked as the white background segments. Table 4 lists the cumulative deviations for the three DOFs where changes are detected, with each exceeding the 6% threshold. During the five subsequent speed changes, the ensemble model, with the assistance of the adaptive weighting mechanism, adjusts to these changes without the need to reactivate the change monitoring mechanism. These periods are marked by light pink background segments in the figure, indicating that the model is ready for online prediction.

The online ensemble models exhibit a high fidelity to the actual data that outperforms the offline model. Specifically, the online ensemble models assimilate new base models and becomes more powerful to adjust to reoccurring concepts or some with the nature of interpolating previous dynamic features. In contrast, the offline model deviated significantly from the simulated data after initial velocity changes. Table 5 lists the RMSE of the predictions and clearly shows that the online ensemble modelling approach is superior to the offline approach. The

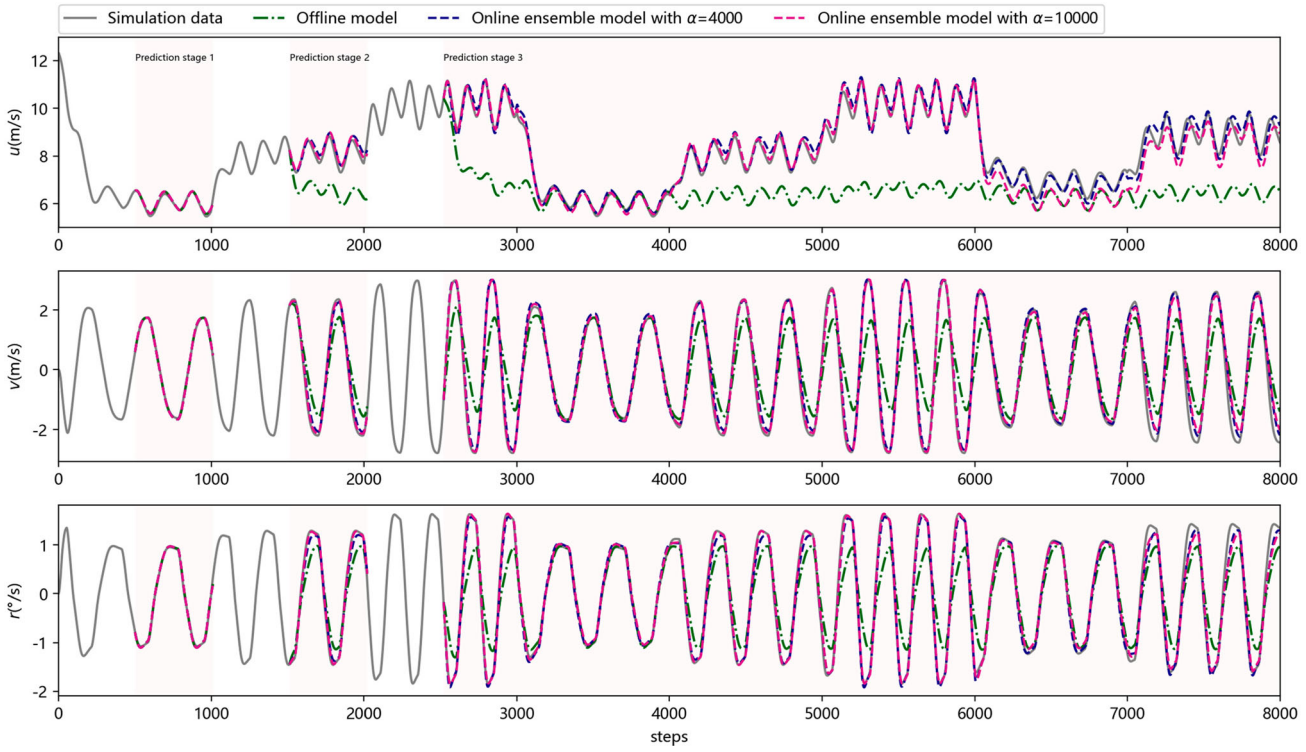

Figure 8. Prediction of the 20°/20° zigzag maneuvers at varying navigation speeds.

Table 5. RMSE for the prediction of variable-speed zigzag.

	Offline model	Online ensemble model with $\alpha = 4000$	Online ensemble model with $\alpha = 10000$
Surge speed	4.3407	0.0525	0.1116
Sway speed	0.6547	0.0388	0.0312
Yaw rate	0.1787	0.0121	0.0095

Table 6. RMSE for predicting reoccurring and unknown concepts of variable-speed zigzag.

	Reoccurring concepts (3000 ~ 6000 steps)		Unknown concepts (6000 ~ 8000 steps)	
	$\alpha = 4000$	$\alpha = 10000$	$\alpha = 4000$	$\alpha = 10000$
Surge speed	0.0462	0.0176	0.0767	0.3263
Sway speed	0.0287	0.0062	0.0689	0.0889
Yaw rate	0.0077	0.0019	0.0227	0.0270

comparative result illustrates the necessity of updating models online, as well as demonstrating the continued accuracy and robustness of the online ensemble models for predicting under concept drift.

The impact of the sensitivity factor α is further analyzed. In the adaptive weighting mechanism, the sensitivity factor α controls the weight allocation to each base model, which may influence the ensemble's performance. Tests are conducted by comparing two online ensemble models with α of 4000 and 10000. Theoretically, with α set to 4000, the weight allocation is relatively moderate, while with α set to 10000, base models with smaller errors are allocated higher weights.

Taking the prediction stage 3 as an example for analysis, the online ensemble models have been established with three base models. These base models correspond to the scenarios under 15.5, 19.8, and 24 knots and are referred to as base models 1, 2, and 3, respectively. In the prediction stage 3, there are three reoccurring concepts from 3000 to 6000 steps with speeds of 15.5, 19.8, and 24 knots, and two unknown concepts from 6000 to 8000 steps with speeds of 18.1 and 22.3 knots. As the speed changes, the weights of the base model need to be adjusted to call the corresponding models to obtain a final prediction.

Figure 9 illustrates the weights of each base model in the surge direction for two online ensemble models from 3000 to 8000 steps. The w_1, w_2 and w_3 denote the weights of the base model 1, base model 2 and base model 3, respectively. In addition, Table 6 presents the RMSE of two sets of online ensemble models for reoccurring and unknown concepts of variable-speed zigzag test.

For the first three reoccurring concepts, both the corresponding base model and other base models contribute to a certain extent when α is set to 4000; however, with α of 10000, only the base model for the specific speed is active. In comparison, the latter seems more reasonable. According to Figure 8 and Table 6, the model with α of 10000 is indeed more accurate, while the model with α of 4000 has a small prediction bias, which is generally acceptable. For the latter two unknown concepts, the

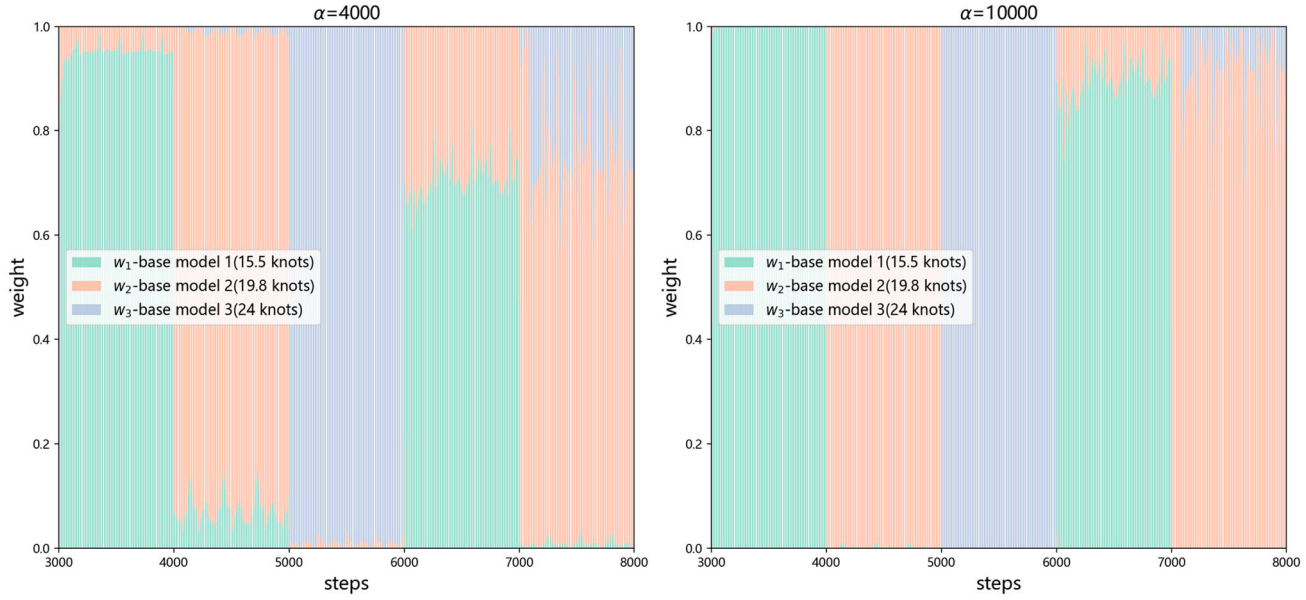

Figure 9. The weights of the base models of variable-speed zigzag from 3000 to 8000 steps.

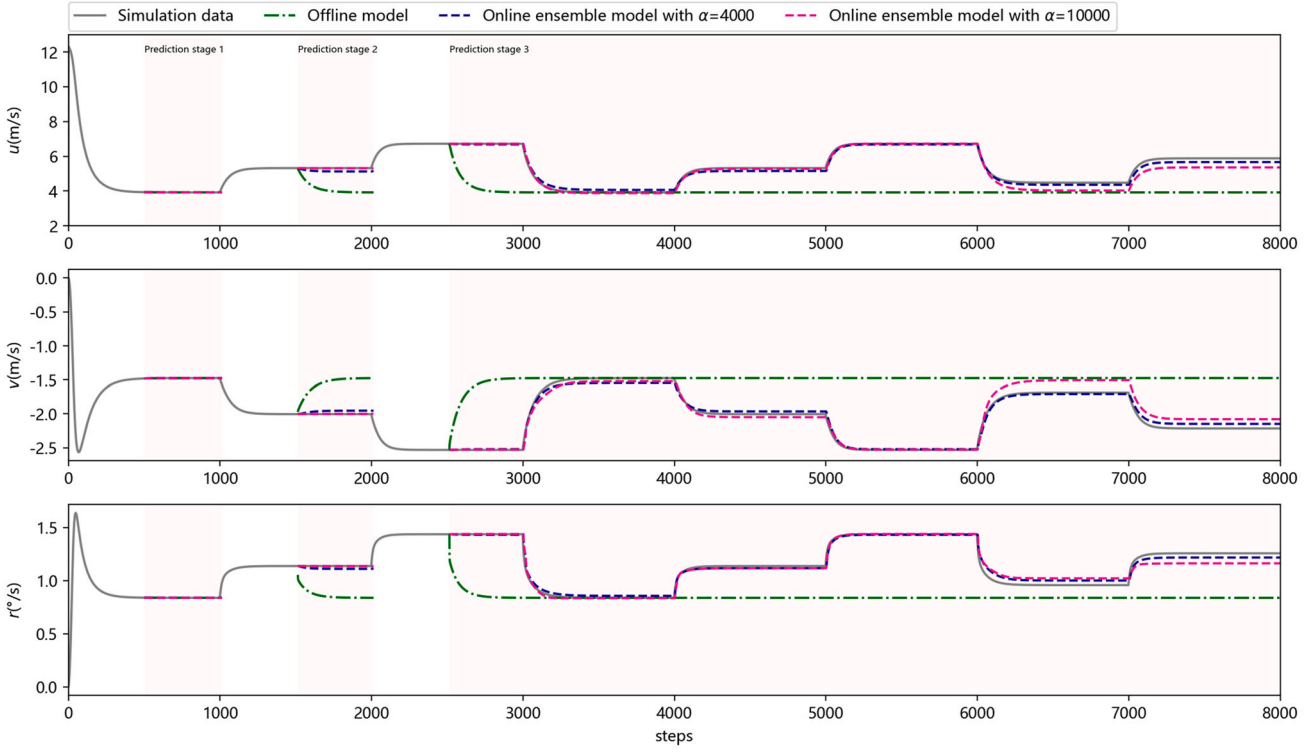

Figure 10. Prediction of the 30° turning maneuvers at varying navigation speeds.

final prediction is a combination of the base models for the two adjacent speeds, which is intuitively consistent. Notably, the weight allocation of base model is more balanced when α is 4000 than α is 10000. As seen in Figure 8 and Table 6, the models with α set to 4000 yield more accurate prediction and lower RMSE. This indicates that the sensitivity of the weight allocation at α of 10000 is somewhat over high, resulting in the allocation not being reasonable enough.

The result demonstrates that α plays a key role in balancing the ability of online ensemble models to predict both known and the unknown concepts. A large α allows the model to adapt to reoccurring concepts, but it is less effective in adapting to unknown concepts. Conversely, a small α enhances the model's adaptability to unknown concepts, but this may compromise the model's accuracy in predicting reoccurring concepts.

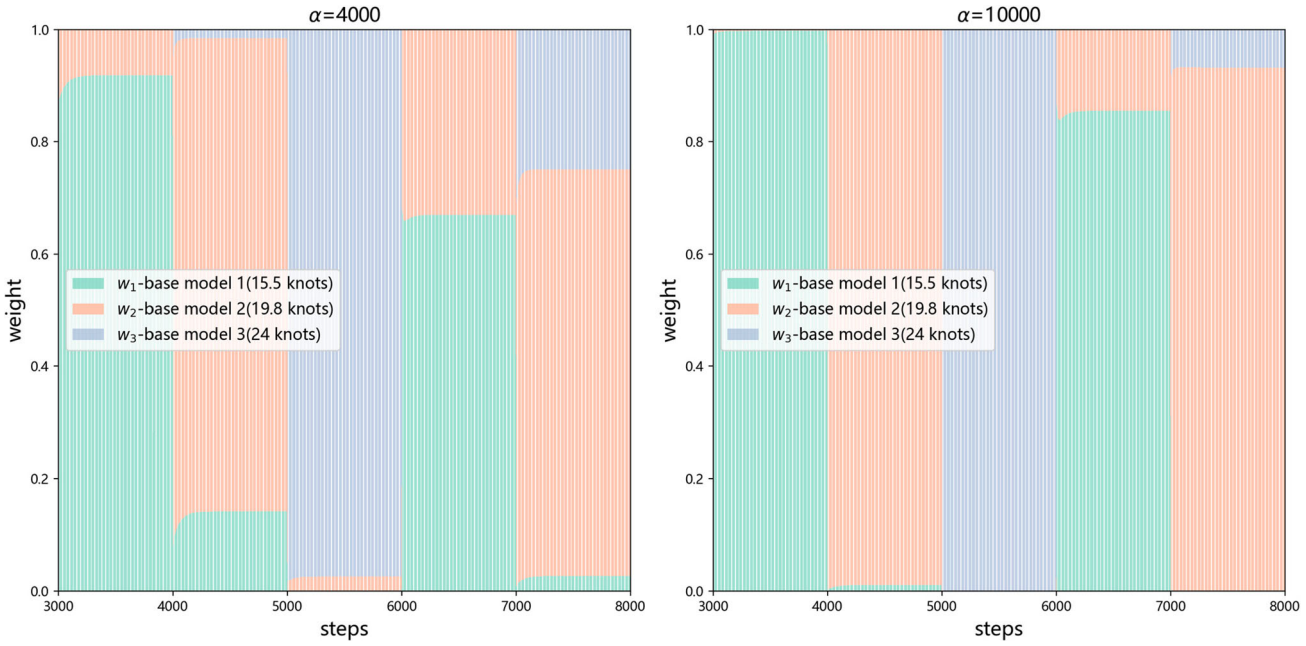

Figure 11. The weights of the base models of variable-speed turning from 3000 to 8000 steps.

Table 7. Changes detected in variable-speed turning.

Order	Time step for the change detected	E_u^t	E_v^t	E_r^t
1	1012	0.0711	0.0622	0.1469
2	2013	0.0687	0.0632	0.1300

Table 8. RMSE for prediction of variable-speed turning.

	Offline Model	Online Model 1	Online Model 2
Surge speed	2.6977	0.0198	0.0698
Sway speed	0.3814	0.0019	0.0083
Yaw rate	0.1260	0.0009	0.0021

Figure 10 shows the prediction results of the 30° turning maneuvers at varying navigation speeds. In variable-speed turning test, the changes are also detected twice and then the prediction process is divided into three stages. Table 7 presents the number of steps for which changes are detected as well as the cumulative deviations in the three DOFs. As the changes are detected, the expansion of base models occurs, thereby extending the capabilities of the online ensemble model. The RMSE presented in Table 8 demonstrates that the online ensemble models exhibit superior performance than the offline model.

Figure 11 shows the weights of each base model in the surge direction for the two online ensemble models in the variable-speed turning test from 3000 to 8000 steps. The w_1, w_2 and w_3 denotes the weight of the base model 1, base model 2 and base model 3 established at 15.5, 19.8, and 24.0 knots, respectively. The predictions of reoccurring concepts range from 3000 to 6000 steps, and the predictions of unknown concepts range from 6000 to 8000 steps. Compared to the variable-speed zigzag test, the weight changes are smoother due to the low frequency changes of steering angles. Table 9 presents the RMSE of two online ensemble models for predicting reoccurring and unknown concepts of the variable-speed turning test. The same conclusion can be drawn that extreme weight allocation has great performance on reoccurring concepts, while moderate weight allocation can improve the generalization performance of the ensemble. The error sensitivity factor α serves to balance the impact of predictions for both reoccurring and unknown concepts, and the appropriate α should effectively harmonize this effect. Testing reveals that the α values ranging from 4000 to 6000 yield comparable outcomes, implying an appropriate α lies within a certain range. In practice, the hyperparameter selection can be initially guided by expert knowledge. Alternatively, it can be determined using techniques like grid search or cross-validation.

Table 9. RMSE for predicting reoccurring and unknown concepts of variable-speed zigzag.

	Reoccurring concepts (3000 ~ 6000steps)		Unknown concepts (6000 ~ 8000steps)	
	$\alpha = 4000$	$\alpha = 10000$	$\alpha = 4000$	$\alpha = 10000$
Surge speed	0.0168	0.0018	0.0298	0.2235
Sway speed	0.0020	0.0017	0.0025	0.0242
Yaw rate	0.0003	0.0002	0.0018	0.0064

In summary, the results validate the effectiveness of the adaptive weighted ensemble learning framework in the online prediction of dynamic changes in ship maneuvers. The case study of ship dynamic changes due to

varying sailing speeds demonstrates the feasibility of the proposed method. This provides the potential for further testing of the approach under varying environmental conditions or on actual ships. Further research deserves to be studied, such as the exclusion mechanism of base models and the way to enhance the generalizability of base models. The online ensemble models constructed in this study not only ensure accurate predictions for reoccurring and some unknown concept drift, but also achieve a certain degree of autonomy, thus avoiding frequent manual recalibration. With the proposed framework, the model's capability can be gradually enhanced with the accumulation of data or the extension of the ship voyage time. Thus, accurate and generalizable online predictions can be provided for applications such as digital twins in the future.

5. Conclusions

This paper has described an adaptive weighted ensemble learning framework to address the concept drift in vehicle dynamics. The framework has a rapid adaptation capability for reoccurring concepts and can consistently update models to accommodate unknown concept drifts. The case studies have preliminarily validated the feasibility of the modelling strategy and indicated that the ensemble model can expand the scope of the model capabilities through interpolation. Furthermore, this framework exhibits potential for wider utilization in addressing different concept drift such as varying payloads or external environmental disturbances. Since the adjustment of the ensemble model is driven by the online prediction error, the proposed method is especially suitable for tasks that demand precise real-time motion prediction, such as in digital twins. In the era of big data, this approach can gradually enhance the capacity of the ensemble model by accumulating a wider range of scenario data. Consequently, there is a possibility of establishing an all-in-one model that can handle multiple scenarios effectively. Future work will involve the detailed design of strategies that balances the ability of base models and computational efficiency, as well as conducting application studies on actual ships.

Disclosure statement

No potential conflict of interest was reported by the author(s).

Funding

This research was funded by the National Natural Science Foundations of China under Grant [52101361].

Data availability statement

The data available from the corresponding author on reasonable request.

ORCID


Zihao Wang http://orcid.org/0000-0002-0035-1789

References

Chen, L. J., Yang, P. Y., Li, S. G., Liu, K. Z., Wang, K., & Zhou, X. W. (2023). Online modeling and prediction of maritime autonomous surface ship maneuvering motion under ocean waves. *Ocean Engineering*, *276*, 114183. https://doi.org/10.1016/j.oceaneng.2023.114183

Gama, J., Žliobaitė, I., Bifet, A., Pechenizkiy, M., & Bouchachia, A. (2014). A survey on concept drift adaptation. *ACM Computing Surveys*, *46*(4), 1–37. https://doi.org/10.1145/2523813

Gomes Soares, S., & Araújo, R. (2015). An on-line weighted ensemble of regressor models to handle concept drifts. *Engineering Applications of Artificial Intelligence*, *37*, 392–406. https://doi.org/10.1016/j.engappai.2014.10.003

Hatledal, L. I., Skulstad, R., Li, G., Styve, A., & Zhang, H. (2020). Co-Simulation as a fundamental technology for twin ships. *Modeling, Identification and Control*, *41*(4), 297–311. https://doi.org/10.4173/mic.2020.4.2

Kadlec, P., & Gabrys, B. (2011). Local learning-based adaptive soft sensor for catalyst activation prediction. *Journal of American Institute of Chemical Engineers*, *57*(5), 1288–1301. https://doi.org/10.1002/aic.12346

Kaneko, H., & Funatsu, K. (2014). Adaptive soft sensor based on online support vector regression and Bayesian ensemble learning for various states in chemical plants. *Chemometrics and Intelligent Laboratory Systems*, *137*, 57–66. https://doi.org/10.1016/j.chemolab.2014.06.008

Lan, J. F., Zheng, M., Chu, X. M., & Ding, S. G. (2023). Parameter prediction of the non-linear nomoto model for different ship loading conditions using support vector regression. *Journal of Marine Science and Engineering*, *11*(5), 903. https://doi.org/10.3390/jmse11050903

Liu, Y., Zou, L., Zou, Z. J., & Guo, H. P. (2018). Predictions of ship maneuverability based on virtual captive model tests. *Engineering Applications of Computational Fluid Mechanics*, *12*(1), 334–353. https://doi.org/10.1080/19942060.2018.1439773

Lu, J., Liu, A. J., Dong, F., Gu, F., Gama, J., & Zhang, G. Q. (2018). Learning under concept drift: A review. *IEEE Transactions on Knowledge and Data Engineering*, 1–1. https://doi.org/10.1109/TKDE.2018.2876857

Nielsen, R. E., Papageorgiou, D., Nalpantidis, L., Jensen, B. T., & Blanke, M. (2022). Machine learning enhancement of manoeuvring prediction for ship digital twin using full-scale recordings. *Ocean Engineering*, *257*, 111579. https://doi.org/10.1016/j.oceaneng.2022.111579

Okuda, R., Yasukawa, H., & Matsuda, A. (2023). Validation of maneuvering simulations for a KCS at different forward speeds using the 4-DOF MMG method. *Ocean Engineering*, *284*, 115174. https://doi.org/10.1016/j.oceaneng.2023.115174

Ouyang, Z. L., & Zou, Z. J. (2021). Nonparametric modeling of ship maneuvering motion based on Gaussian process regression optimized by genetic algorithm. *Ocean Engineering*, *238*, 109699. https://doi.org/10.1016/j.oceaneng.2021.109699

PANDA, J. P. (2023). Machine learning for naval architecture, ocean and marine engineering. *Journal of Marine Science and Technology*, *28*(1), 1–26. https://doi.org/10.1007/s00773-022-00914-5

Pei, T. Q., Yu, C. Y., Zhong, Y. M., & Lian, L. (2023). Adaptive event-triggered mechanism-based online system identification framework for marine craft. *Ocean Engineering*, *278*, 114572. https://doi.org/10.1016/j.oceaneng.2023.114572

Polikar, R. (2012). *Ensemble Machine Learning: Methods and Applications* (pp. 1–34). https://doi.org/10.1007/978-1-4419-9326-71

Silva, K. M., & Maki, K. J. (2022). Data-Driven system identification of 6-DoF ship motion in waves with neural networks. *Applied Ocean Research*, *125*, 103222. https://doi.org/10.1016/j.apor.2022.103222

Son, K. H., & Nomoto, K. (1981). On the coupled motion of steering and rolling of a high-speed container ship. *Naval Architecture and Ocean Engineering*, *150*, 232–244. https://doi.org/10.2534/jjasnaoe1968.1981.150_232

Wakita, K., Maki, A., Umeda, N., Miyauchi, Y., Shimoji, T., Rachman, D. M., & Akimoto, Y. (2022). On neural network identification for Low-speed ship maneuvering model. *Journal of Marine Science and Technology*, *27*(1), 772–785. https://doi.org/10.1007/s00773-021-00867-1

Wang, S. S., Wang, L. J., Im, N., Zhang, W. D., & Li, X. J. (2022). Real-Time parameter identification of ship maneuvering response model based on nonlinear Gaussian filter. *Ocean Engineering*, *247*, 110471. https://doi.org/10.1016/j.oceaneng.2021.110471

Wang, T. T., Li, G. Y., Hatledal, L. I., Skulstad, R., AEsoy, V., & Zhang, H. X. (2022). Incorporating approximate dynamics into data-driven calibrator: A representative model for ship maneuvering prediction. *IEEE Transactions on Industrial Informatics*, *18*(3), 1781–1789. https://doi.org/10.1109/TII.2021.3088404

Wang, T. T., Li, G. Y., Wu, B. H., Æsøy, V., & Zhang, H. X. (2021). Parameter identification of ship manoeuvring model under disturbance using support vector machine method. *Ships and Offshore Structures*, *16*(sup1), 13–21. https://doi.org/10.1080/17445302.2021.1927600

Wang, T. T., Skulstad, R., Kanazawa, M., Hatledal, L. I., Li, G. Y., & Zhang, H. X. (2022). Adaptive data-driven predictor of ship maneuvering motion under varying ocean environments. In T. Margaria, & B. Steffen (Eds.), *Proceedings of the leveraging applications of formal methods, verification and validation. Practice* (pp. 110–125). Springer Nature Switzerland.

Wang, Z. H., Xu, H. T., Xia, L., Zou, Z. J., & Guedes Soares, C. (2020). Kernel-Based support vector regression for nonparametric modeling of ship maneuvering motion. *Ocean Engineering*, *216*, 107994. https://doi.org/10.1016/j.oceaneng.2020.107994

Wang, Z. H., Zou, Z. J., & Guedes Soares, C. (2019). Identification of ship manoeuvring motion based on Nu-support vector machine. *Ocean Engineering*, *183*, 270–281. https://doi.org/10.1016/j.oceaneng.2019.04.085

Wu, B. H., Li, G. Y., Zhao, L. M., Aandahl, H. I. J., Hildre, H. P., & Zhang, H. X. (2022). Navigating patterns analysis for onboard guidance support in crossing collision-avoidance operations. *IEEE Intelligent Transportation Systems Magazine*, *14*(3), 62–77. https://doi.org/10.1109/MITS.2021.3108473

Xiang, G., Xiang, X., & Datla, R. (2023). Numerical study of a novel small waterplane area USV advancing in calm water and in waves using the higher-order rankine source method. *Engineering Applications of Computational Fluid Mechanics*, *17*(1), 2241892. https://doi.org/10.1080/19942060.2023.2241892

Xu, H. T., Hinostroza, M. A., Hassani, V., & Guedes Soares, C. (2019). Real-Time parameter estimation of a nonlinear vessel steering model using a support vector machine. *Journal of Offshore Mechanics and Arctic Engineering-Transactions of the Asme*, *141*(6), 061606. https://doi.org/10.1115/1.4043806

Xue, Y. F., Liu, Y. J., Xue, G., & Chen, G. (2021). Identification and prediction of ship maneuvering motion based on a Gaussian process with uncertainty propagation. *Journal of Marine Science and Engineering*, *9*(8), 804. https://doi.org/10.3390/jmse9080804

Yasukawa, H., Himaya, A. N., Hirata, N., & Matsuda, A. (2022). Simulation study of the effect of loading condition changes on the maneuverability of a container ship. *Journal of Marine Science and Technology*, https://doi.org/10.1007/s00773-022-00908-3

Yu, Y. H., Wang, Z. H., Qu, D., Song, R., & Peng, Y. (2023, June 11). Online modeling of ship maneuvering motion with varying loading conditions. In Proceedings of the Volume 5: Ocean Engineering; American Society of Mechanical Engineers: Melbourne, Australia, p. V005T06A047.

Yue, J. W., Liu, L., Gu, N., Peng, Z. H., Wang, D., & Dong, Y. (2022). Online adaptive parameter identification of an unmanned surface vehicle without persistency of excitation. *Ocean Engineering*, *250*, 110232. https://doi.org/10.1016/j.oceaneng.2021.110232

Appendix A

The ship dynamic model and parametric identification framework mainly refer to (Wang et al., 2019). The equations for ship maneuvering motion can be described as a 3-DOF model that includes surge, sway and yaw:

$$\begin{bmatrix} m-X_{\dot{u}} & 0 & 0 \\ 0 & m-Y_{\dot{v}} & mx_G-Y_{\dot{r}} \\ 0 & mx_G-N_{\dot{v}} & I_z-N_{\dot{r}} \end{bmatrix} \begin{bmatrix} \dot{u} \\ \dot{v} \\ \dot{r} \end{bmatrix} = \begin{bmatrix} f_1 \\ f_2 \\ f_3 \end{bmatrix}, \quad \text{(A1)}$$

$$\begin{cases} f_1 = X_u\Delta u + X_{uu}\Delta u^2 + X_{uuu}\Delta u^3 \\ +X_{vv}v^2 + X_{rr}r^2 + X_{rv}rv + X_{\delta\delta}\delta^2 \\ +X_{u\delta\delta}\Delta u\delta^2 + X_{v\delta}v\delta + X_{uv\delta}\Delta uv\delta \\ f_2 = Y_0 + Y_u\Delta u + Y_{uu}\Delta u^2 + Y_v v + Y_r r + Y_{vvv}v^3 \\ +Y_{vvr}v^2 r + Y_{vu}v\Delta u \\ +Y_{ru}r\Delta u + Y_\delta\delta + Y_{\delta\delta\delta}\delta^3 + Y_{u\delta}\Delta u\delta + Y_{uu\delta}\Delta u^2\delta \\ +Y_{v\delta\delta}v\delta^2 + Y_{vv\delta}v^2\delta \\ f_3 = N_0 + N_u\Delta u + N_{uu}\Delta u^2 + N_v v + N_r r \\ +N_{vvv}v^3 + N_{vvr}v^2 r + N_{vu}v\Delta u \\ +N_{ru}r\Delta u + N_\delta\delta + N_{\delta\delta\delta}\delta^3 \\ +N_{u\delta}\Delta u\delta + N_{uu\delta}\Delta u^2\delta + N_{v\delta\delta}v\delta^2 + N_{vv\delta}v^2\delta \end{cases}, \quad \text{(A2)}$$

where m is the mass of the ship, u, v, r and δ are the surge speed, sway speed, yaw rate and rudder angle, respectively. I_z is the moment of inertia, x_G is the ordinate of the ship's centre of gravity. X_u, Y_r and N_v etc. are the hydrodynamic coefficients. Y_0, N_0 are the hydrodynamic force in the direction of y-axis and the

yaw moment about z-axis during the straight forward motion with constant speed. Δu is the disturbing quantity of the surge speed.

In the state of the straight forward motion with constant speed: $u_0 = U_0$, $\Delta u = u - u_0$, $v_0 = r_0 = \delta_0 = \dot{u}_0 = \dot{v}_0 = \dot{r}_0 = 0$. And the resultant speed: $U = [(u_0 + \Delta u)^2 + v^2]^{1/2}$.

Discretizing the continuous equations of motion by Euler's method:

$$\dot{u}(k) = \frac{\Delta u(k+1) - \Delta u(k)}{h} \tag{A3}$$

$$\dot{v}(k) = \frac{v(k+1) - v(k)}{h} \tag{A4}$$

$$\dot{r}(k) = \frac{r(k+1) - r(k)}{h} \tag{A5}$$

where h is the sampling interval, k and $k+1$ are the adjacent sampling time steps.

Combining Equations (A1) $\sim$ (A5), the following formulas can be obtained:

$$\begin{aligned}\Delta u(k+1) - \Delta u(k) = {} & a_1 \Delta u(k) U(k) + a_2 \Delta u^2(k) \\ & + \frac{a_3 \Delta u^3(k)}{U(k)} + a_4 v^2(k) + a_5 r^2(k) \\ & + a_6 v(k) r(k) + a_7 \delta^2(k) U^2(k) \\ & + a_8 \Delta u(k) \delta^2(k) U(k) \\ & + a_9 v(k) \delta(k) U(k) \\ & + a_{10} \Delta u(k) v(k) \delta(k),\end{aligned} \tag{A6}$$

$$\begin{aligned}v(k+1) - v(k) = {} & b_1 U^2(k) + b_2 \Delta u(k) U(k) + b_3 \Delta u^2(k) \\ & + b_4 v(k) U(k) + b_5 r(k) U(k) + \frac{b_6 v^3(k)}{U(k)} \\ & + \frac{b_7 v^2(k) r(k)}{U(k)} + b_8 v(k) \Delta u(k) \\ & + b_9 r(k) \Delta u(k) + b_{10} \delta(k) U^2(k) \\ & + b_{11} \delta^3(k) U^2(k) \\ & + b_{12} \Delta u(k) \delta(k) U(k) + b_{13} \Delta u^2(k) \delta(k) \\ & + b_{14} v(k) \delta^2(k) U(k) + b_{15} v^2(k) \delta(k),\end{aligned} \tag{A7}$$

$$\begin{aligned}r(k+1) - r(k) = {} & c_1 U^2(k) + c_2 \Delta u(k) U(k) + c_3 \Delta u^2(k) \\ & + c_4 v(k) U(k) + c_5 r(k) U(k) + \frac{c_6 v^3(k)}{U(k)} \\ & + \frac{c_7 v^2(k) r(k)}{U(k)} + c_8 v(k) \Delta u(k) \\ & + c_9 r(k) \Delta u(k) + c_{10} \delta(k) U^2(k) \\ & + c_{11} \delta^3(k) U^2(k) \\ & + c_{12} \Delta u(k) \delta(k) U(k) + c_{13} \Delta u^2(k) \delta(k) \\ & + c_{14} v(k) \delta^2(k) U(k) + c_{15} v^2(k) \delta(k)\end{aligned} \tag{A8}$$

The above equations can be further abbreviated as:

$$\Delta u(k+1) - \Delta u(k) = AP, \tag{A9}$$

$$v(k+1) - v(k) = BN, \tag{A10}$$

$$r(k+1) - r(k) = CZ, \tag{A11}$$

where P, N, and Z are the variable vectors, which can be expressed as:

$$\begin{cases} P = [\Delta u(k) U(k), \Delta u^2(k), \dfrac{\Delta u^3(k)}{U(k)}, v^2(k), r^2(k), v(k) r(k), \\ \delta^2(k) U^2(k), \Delta u(k) \delta^2(k) U(k), v(k) \delta(k) U(k), \\ \Delta u(k) v(k) \delta(k)]^{\mathrm{T}}_{1 \times 10} \\ N = Z = [U^2(k), \Delta u(k) U(k), \Delta u^2(k), v(k) U(k), r(k) U(k), \\ \dfrac{v^3(k)}{U(k)}, \dfrac{v^2(k) r(k)}{U(k)}, v(k) \Delta u(k), r(k) \Delta u(k), \delta(k) U^2(k), \\ \delta^3(k) U^2(k), \Delta u(k) \delta(k) U(k), \Delta u^2(k) \delta(k), v(k) \delta^2(k) U(k), \\ v^2(k) \delta(k)]^{\mathrm{T}}_{1 \times 15}, \end{cases} \tag{A12}$$

A, B and C are the parameter vectors to be identified:

$$\begin{cases} A = [a_1, a_2, a_3, a_4, a_5, a_6, a_7, a_8, a_9, a_{10}]_{1 \times 10} \\ B = [b_1, b_2, b_3, b_4, b_5, b_6, b_7, b_8, b_9, b_{10}, b_{11}, b_{12}, b_{13}, b_{14}, b_{15}]_{1 \times 15} \\ C = [c_1, c_2, c_3, c_4, c_5, c_6, c_7, c_8, c_9, c_{10}, c_{11}, c_{12}, c_{13}, c_{14}, c_{15}]_{1 \times 15} \end{cases} \tag{A13}$$

For multiple linear regression, the regression equation is expressed as:

$$y = X\hat{\beta}, \tag{A14}$$

X is the eigenvalue matrix, $\hat{\beta}$ is the parameter vector, and y is the labelled value vector, expressed respectively:

$$X = \begin{bmatrix} 1 & x_{11} & \cdots & x_{1n} \\ 1 & x_{21} & \cdots & x_{2n} \\ \cdots & \cdots & \cdots & \cdots \\ 1 & x_{m1} & \cdots & x_{mn} \end{bmatrix}, \hat{\beta} = \begin{bmatrix} \hat{\beta}_0 \\ \hat{\beta}_1 \\ \cdots \\ \hat{\beta}_n \end{bmatrix}, y = \begin{bmatrix} y_1 \\ \cdots \\ y_m \end{bmatrix}, \tag{A15}$$

where m is the number of samples, n is the number of features.

The loss function is defined as:

$$J(\hat{\beta}) = \sum_{i=1}^{m} \left| y_i - \left(\hat{\beta}_0 + \sum_{j=1}^{n} x_{ij} \hat{\beta}_j \right) \right|^2, \tag{A16}$$

Solve for the parameter vector $\hat{\beta}$ by minimizing $J(\hat{\beta})$, which is derived for $\hat{\beta}$ and made equal to zero:

$$\frac{\partial J(\hat{\beta})}{\partial \hat{\beta}} = X^T X \hat{\beta} - X^T y = 0, \tag{A17}$$

The parameter vector is obtained from Equation (A17):

$$\hat{\beta} = (X^T X)^{-1} X^T y \tag{A18}$$